# Model Predictive Current Control of a Seven-phase Voltage Source Inverter

Atif Iqbal[1] Senior Member IEEE, Khaleequr Rahman, Mostafa Mosa*, Ahmad Anad Abdullah, Haitham Abu-Rub* Senior Member IEEE, SK. Moin Ahmed*, Member IEEE
Department of Electrical Engineering, Qatar University, Doha, Qatar
*Electrical & Computer Engineering Program, Texas A&M University at Qatar, Doha, Qatar

***Abstract*-The paper elaborate finite set model based predictive current control of a seven-phase voltage source inverter. The current control is carried out considering a finite set of control actions. The space vector model of a seven-phase voltage source inverter (VSI) yields $2^7 = 128$ space voltage vectors, with 126 active and two zero vectors. The control method described in this paper discard some switching states from the whole set and employs reduced number of switching states to track the commanded current. Three sets of space vectors are used for switching actuation, in one case only 15 vectors are used (14 active and one zero), in second case 29 vectors are used (28 active and one zero) and finally 43 vectors (42 active and one zero) are employed. Optimal algorithm is employed to find the vector which minimizes the chosen cost function. The effect of selecting the cost function, the number of space vectors and the sampling time is investigated and reported. The developed technique is tested for RL load using simulation and experimental approaches.**

***Keywords:* Multi-phase, seven-phase, model predictive control, space vector, PWM, Total harmonic distortion.**

## I. Introduction

In power electronic converter, the current control is considered as one of the important and crucial issue. Many literature reported current control issues and several techniques are proposed over years [1]. Traditional methods of current control are Hysteresis based control also called bang-bang control, carrier-based sinusoidal current control and current control based on space vectors approach [2]. Hysteresis current control is most simple method but it gives variable switching frequency and is difficult for digital realization. Ramp comparison PWM technique and space vector PWM approaches yield constant switching frequency operation. Hysteresis control offer variable switching frequency, however, it can be modified to generate constant switching frequency of the inverter legs [3]. Another approach of current control called 'model predictive current control' (MPC) are becoming more popular for applications in power electronics and electric drives. Since power converter generates many switching states and some of them are redundant and may not be useful in obtaining high performance dynamics. Hence, some of the switching states can be rejected and may not be employed for control such control are called 'finite set model predictive control'. This technique has been employed in controlling three-phase power electronics converters and drives [4-9]. Inherently, MPC is computational intensive approach however, due to the advent of fast signal processors and microcontrollers it is now practically realizable approach for power electronic converters and drives. The method of control is also attractive for multiphase motor drives and literature is available on utilizing MPC for five-phase two-level inverter [10, 11], six-phase inverter [12-15] and five-phase three-level NPC inverter [16].

Owing to inherent advantages of multi-phase machine, they are considered mainly in high power drive applications such as ship propulsion, electric and hybrid vehicles, 'more electric aircraft' etc [17]. Proper Pulse Width Modulation control techniques are needed to control the drive system that are supplied by multi-phase inverters. Several PWM techniques are proposed and presented in the literature for multi-phase voltage source inverters [17, 18].

The current control in multi-phase drive system is an extension of three-phase drive such as hysteresis control, carrier-based control, space vector based control and other non-linear controls [17].

This paper proposes finite set model predictive current control of a seven-phase VSI feeding a RL load. The proposed approach is extension of method adopted for a five-phase VSI [10,11]. A seven-phase inverter generates $2^7 = 128$ space vectors and thus there is greater degree of freedom in choosing proper space vector combination for implementing the control algorithm [19]. This paper proposes an algorithm based on a choice of 14 active and one zero, 28 active and one zero and 42 active, and one zero vectors while the total set of vectors are 128. Reduced number of space vector are used since it is easier for the real time implementation. Furthermore in model based predictive current control, choosing cost function is key in meeting control objectives. [7]. Since a seven-phase system when transformed produces vectors in three orthogonal planes d-q, x1-y1, and x2-y2 in seven dimensional space. The vectors in d-q plane generate the working current responsible for torque production if an ac machine is supplied from the inverter while the other two components, that are only limited by the leakage impedance of the machine, generate additional losses. Thus, the aim of the controller should be to eliminate such current components

[1] Dr. Iqbal Is with Electrical Engg. Deptt., Aligarh Muslim University, Aligarh, India and is presently on academic assignment at QU.



© 2013 ACEEE
DOI: 03.LSCS.2013.4.9

produced by unwanted x1-y1 and x2-y2 planes. This is possible by properly choosing the space vectors and the cost functions as elaborated in the paper. The effect of choice of different number of space vectors are investigated. The aim is to obtain lower Total harmonic distortion in the current waveform with good dynamics.

## II. Model Predictive current control

### *A. The Control Strategy*

The current control suggested in this paper is based on the finite set model predictive approach. The power converter yield $2^7$ = 128 switching states, however, for the current control, reduced switching states are utilized and hence called 'finite set' MPC. A block diagram to show the principle of the proposed strategy is depicted in Fig. 1. The discrete load model called 'Predictive Model' is used to pre-calculate the trajectory of the load current in the next sampling interval assuming the known current in the present sample. The pre-calculated current sample is then fed to the optimizer along with the commanded current (obtained from the external user controlled loop). The optimizer calculates the cost function for all the possible switching combinations of the inverter (note that smaller set of vectors are chosen). Thus, it generates the optimal switching state corresponding to the global minimum cost function in each sampling interval and passes it on to the gate drive of the inverter. This is how the optimal current control solution is obtained. The technique of model predictive control concept is different from the traditional pulse width modulation method. In traditional PWM the symmetrical switching patterns are generated and it is ensured that each leg changes the state at-least twice in the same switching interval. This ensure constant switching frequency spectrum of the load current. Contrary to this, in the model predictive control approach there is no fixed switching pattern and hence the spectrum shows variable switching frequency. However, MPC approach is very powerful being simple and intuitive. The controller can incorporate many desired control features and can met several control objectives by simple modification of the cost function. The cost function can incorporate other control features such as reduced switching losses, lower switch stress, number of switch commutation etc.

A seven-phase voltage source inverter yield large number of space vectors (126 active and 2 zero), several possible solutions could exist to implement model predictive control. Many control objectives can be met with flexible control. Nevertheless, in this paper three different solutions are investigated and reported. However, there still remain many more to explore.

### *B. The Cost function*

The choice of the cost function is the most important and crucial step of the model predictive control. An intelligent choice leads to the optimal solution of the control objectives. Thus, the cost function should include all the parameters to be optimized within the imposed constrains. In the current

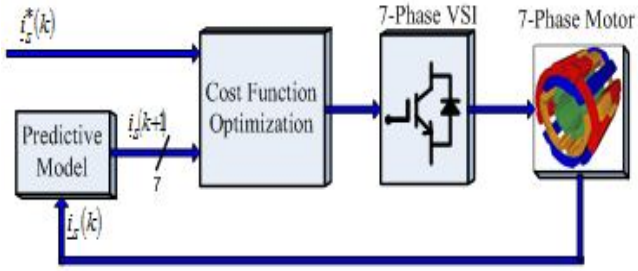



Fig. 1. Model predictive control block schematic

control the most important variable is the current tracking error. Thus the most simple and straight forward choice is the absolute value of the current error. The other choices could be square of the current error, integral of the current error, the rate of change of error etc. In this paper, square of the absolute error is chosen. Specifically in a seven-phase drive system there exist three orthogonal subspaces namely $\alpha$-$\beta$ and $x_1$-$y_1$ and $x_2$-$y_2$. Thus in case of a seven-phase drive system the current errors in all the three planes have to be considered for devising a cost function. In general, for current error, the cost function is given as;

$$\begin{aligned}\hat{g}_{\alpha\beta} &= \left|i^*_{\alpha}(k)-\hat{i}_{\alpha}(k+1)\right|+\left|i^*_{\beta}(k)-\hat{i}_{\beta}(k+1)\right| \\ \hat{g}_{x1y1} &= \left|i^*_{x1}(k)-\hat{i}_{x1}(k+1)\right|+\left|i^*_{y1}(k)-\hat{i}_{y1}(k+1)\right| \\ \hat{g}_{x2y2} &= \left|i^*_{x2}(k)-\hat{i}_{x2}(k+1)\right|+\left|i^*_{y2}(k)-\hat{i}_{y2}(k+1)\right|\end{aligned} \quad (1)$$

The final cost function can be expressed as;

$$J_{\alpha\beta xy} = \left\|\hat{g}_{\alpha\beta}\right\|^2 + \gamma\left\|\hat{g}_{x1y1}\right\|^2 + \delta\left\|\hat{g}_{x2y2}\right\|^2 \quad (2)$$

Where $\|.\|$ denote modulus and $\gamma$ & $\delta$ are tuning parameters that offers degree of freedom to put emphasis on $\alpha-\beta$ or $x_1-y_1$, or $x_2-y_2$ subspaces. Comparative studies are made to emphasize the effect of choice of the tuning parameter on the performance of the controller.

### *C. Seven-phase Inverter Model*

Power circuit topology of a seven-phase VSI feeding a RLE load is shown in Fig. 2. The inverter input DC voltage is regarded further on as being constant. The inverter output phase voltages are denoted in Fig.2 with lower case symbol *(a,b,…,g),* while the leg voltages have symbols in capital letters *(A,B,……,G).* The model of seven-phase VSI is developed in space vector form in [20], assuming an ideal commutation and zero forward voltage drop. A brief review is presented here.

The relationship between the inverter phase-to-neutral voltages and inverter pole voltages is obtained as;

$$\begin{aligned}v_a &= (6/7)v_A-(1/7)(v_B+v_C+v_D+v_E+v_F+v_G) \\ v_b &= (6/7)v_B-(1/7)(v_A+v_C+v_D+v_E+v_F+v_G) \\ v_c &= (6/7)v_C-(1/7)(v_A+v_B+v_D+v_E+v_F+v_G) \\ v_d &= (6/7)v_D-(1/7)(v_A+v_B+v_C+v_E+v_F+v_G)\end{aligned} \quad (3)$$

© 2013 ACEEE
DOI: 03.LSCS.2013.4.9

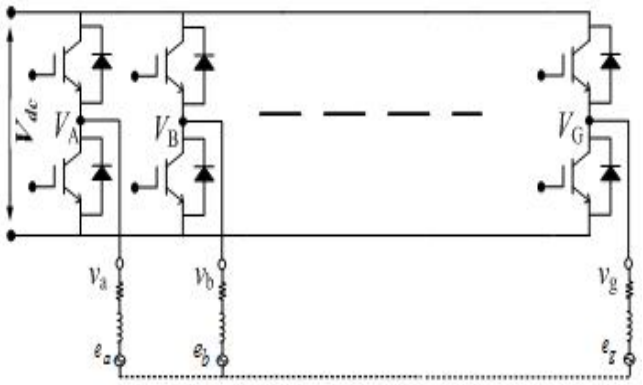



Fig. 2. Power Circuit of a seven-phase VSI

$$v_e = (6/7)v_E - (1/7)(v_A + v_B + v_C + v_D + v_F + v_G)$$

$$v_f = (6/7)v_F - (1/7)(v_A + v_B + v_C + v_D + v_E + v_G)$$

$$v_g = (6/7)v_G - (1/7)(v_A + v_B + v_C + v_D + v_E + v_F)$$

where the inverter pole voltages take the values of $\pm 0.5V_{DC}$.

In general, an *n* phase two level VSI yield a total of $2^n$ number of switching states. Therefore, for a seven-phase VSI, total number of switching states are 128, in which two are zero vectors and the remaining 126 are active vectors. By using decoupling transformation matrix given in (3) each voltage vector can be decomposed into three orthogonal two dimensional subspaces *d-q*, $x_1$-$y_1$ and $x_2$-$y_2$ (assuming isolated neutral and hence no zero sequence component).

In case of a seven-phase VSI, total switching combination of 128 numbers yield same number of switching space voltage vectors. Out of these 128 space voltage vectors, 126 are active and two are zero space vectors and they form nine concentric polygons of fourteen sides in *d-q* plane with zero space vectors at the origin as shown in Fig. 3.

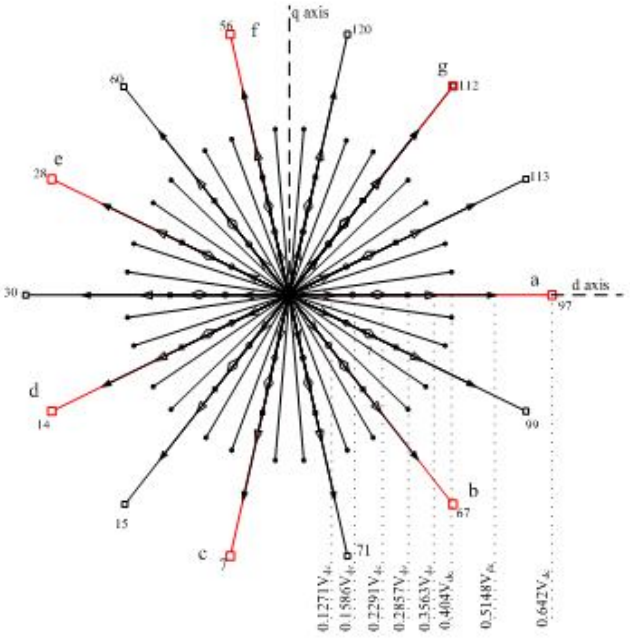



Fig. 3. Phase-to-neutral voltage space voltage vectors (states 0 and 128 are at origin) in *d-q* plane.

However, since a seven-phase system is under consideration, one has to represent the inverter space vectors in a seven-dimensional space. Such a space can be decomposed into three two-dimensional sub-spaces (*d-q*, $x_1$-$y_1$ and $x_2$-$y_2$) and one single-dimensional sub-space (zero-sequence). Since the load is assumed to be star-connected with isolated neutral point, zero-sequence cannot be excited and it is therefore sufficient to consider only three two-dimensional sub-spaces, *d-q*, $x_1$-$y_1$ and $x_2$-$y_2$. Inverter voltage space vector in *d-q* sub-space is given with [20],

$$\underline{v}_{dq} = (2/7)\left(v_a + av_b + a^2v_c + a^3v_d + a^{*3}v_e + a^{*2}v_f + a^*v_g\right) \quad (4a)$$

where $a = e^{j2\pi/7}$, $a^2 = e^{j4\pi/7}$, $a^3 = e^{j6\pi/7}$, $a^{*3} = e^{-j6\pi/7}$, $a^{*2} = e^{-j4\pi/7}$, $a^* = e^{-j2\pi/7}$ Inverter voltage space vectors in the second two-dimensional sub-space ($x_1$-$y_1$) and the third two-dimensional sub-space ($x_2$-$y_2$) are determined with,

$$\underline{v}_{x1y1} = (2/7)\left(v_a + a^2v_b + a^4v_c + a^6v_d + av_e + a^3v_f + a^5v_g\right)$$

$$\underline{v}_{x2y2} = (2/7)\left(v_a + a^3v_b + a^6v_c + a^2v_d + a^5v_e + av_f + a^4v_g\right) \quad (4b)$$

The phase voltage space vectors in two orthogonal planes, obtained using (1), are shown in Figs. 4-5.

It can be seen from Figs. 2, 3a and 3b that the outer most i.e. first, second, third, fourth, fifth, sixth, seventh, and eighth tetra-decagons space vectors of the $d-q$ plane map into the sixth, eighth, third, second, fifth, seventh, first and fourth of the tetra-decagon of the $x_1 - y_1$ plane respectively; and seventh, fourth, third, eighth, fifth, first, sixth and second of the tetra-Decagon of the $x_2 - y_2$ plane respectively. To show this mapping same symbolic representation are used for the same group of space vectors. Further, it is observed from the above mapping that the phase sequence *a,b,c,d,e,f & g* of plane corresponds to *a,c,e,g,b,d,f* of plane (third harmonic) and *a,d,g,c,f,b,e* of plane (fifth harmonic), respectively.

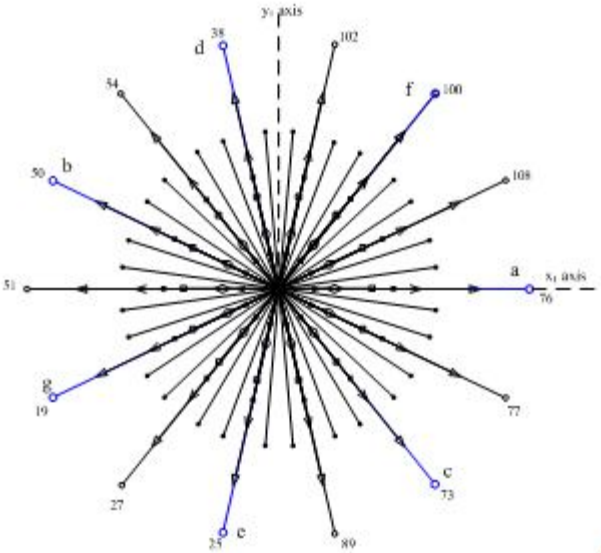



Fig. 4. Phase-to-neutral voltage space vectors for states 1-128.(states0-128 are at origin) in $x_1$-$y_1$ plane



© 2013 ACEEE

DOI: 03.LSCS.2013.4.9

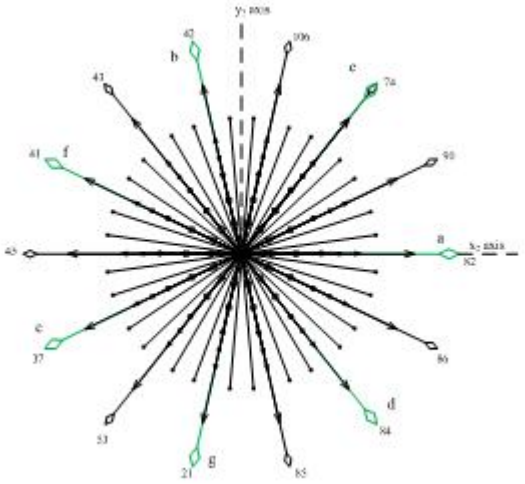


Fig. 5. Phase-to-neutral voltage space vectors for states 1-128.(states0-128 are at origin) in $x_2$-$y_2$ plane

*D. Discrete Load Model*

The load is assumed as a seven-phase RL (Resistance and, inductance). The discrete time model of the load suitable for current prediction is obtained from [6,7];

$$\hat{\underline{i}}(k+1) = \frac{T_s}{L}(\underline{v}(k)) + \underline{i}(k)\left(1 - \frac{RT_s}{L}\right) \qquad (5)$$

Where $R$ and $L$ are the resistance and inductance of the load, $T_s$ is the sampling interval, $\underline{i}$ is the load current space vector, $\underline{v}$ is the inverter voltage space vector used as a decision variable.

## III. Simulation results

Simulation is carried out for three possible solutions in Matlab/Simulink environment, nevertheless, many more can be evaluated. Investigation is done at first using outer large vectors set (14 active vectors and one zero vector) from Fig. 6. At first the effect of choice of tuning parameter of the cost function is evaluated. The cost function is such that it minimizes current tracking error only in $\alpha$-$\beta$ plane leaving the other two planes vectors freely flowing. This followed by using a cost function which takes into account the current tracking error minimization in all the three planes i.e. in $\alpha$-$\beta$, $x_1$-$y_1$ and $x_2$-$y_2$ planes. This is followed by investigation into using higher number of switching vectors and one addition set of vectors is included. Thus altogether 29 vectors are employed (28 active and 1 zero). The sampling time $T_s$ is kept equal to 20 µsec which is reasonable for practical implementation. Nevertheless, this is another degree of freedom that can be further varied. The fundamental frequency of the sinusoidal reference current is chosen as 50 Hz. The load parameters are $R$ = 75 Ω, $L$ = 33 mH and E = 0, and the dc link voltage is kept at $V_{dc}$ = 600 V. The six-phase reference current amplitude is at first kept at 2.0 A and then is stepped up to 4.0 A and further reduced to 1.0 A. The optimization algorithm is implemented using 's' function of the Matlab.

*A. Using $\gamma = 0, \delta = 0$ (current tracking in d-q Plane only) with 15 vectors*

The simulation is carried out with fourteen active and one zero vector while the cost function minimizes current tracking error in α-β plane only. This is achieved by keeping the tuning parameters $\gamma = 0, \delta = 0$. This results in a control action only on one plane while leaving the second (x1-y1) and third (x2-y2) planes uncontrolled. The sampling time of the algorithm is kept at 20 µsec, which is reasonable for processor handling. The resulting waveforms are shown in Fig. 7-8 for phase 'a' actual and reference current, the transformed currents (d-q, x1-y1 and x2-y2), the spectrum of phase 'a' current. The vectors that are used for implementing the model predictive control is elaborated in Fig. 4, where the vectors in all three planes are depicted.

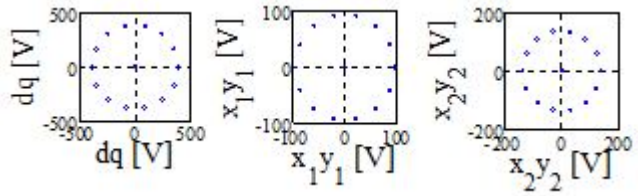



Fig. 6. Fourteen large vectors and their mapping

The actual current follows well the refernce current, however, the shape of the actual current is not sinuosoidal since the control is performed only in d-q plane. The other two plane vectors are free to create low order harmonics as seen from Fig. 6 where the Total harmonic distortion is 28.32% considering the computation upto 50th harmonics. The highest low order harmonics are 3rd (27.5%) and fifth (11.3%).

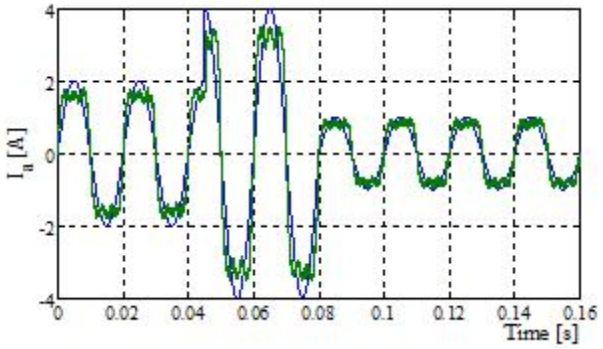



Fig. 7a. Actual and reference phase 'a' current

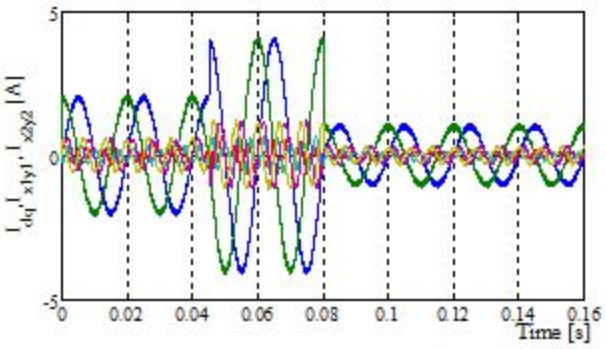



Fig. 7b. Transformed currents in d-q, x1-y1 and x2-y2 planes



© 2013 ACEEE

DOI: 03.LSCS.2013.4.9

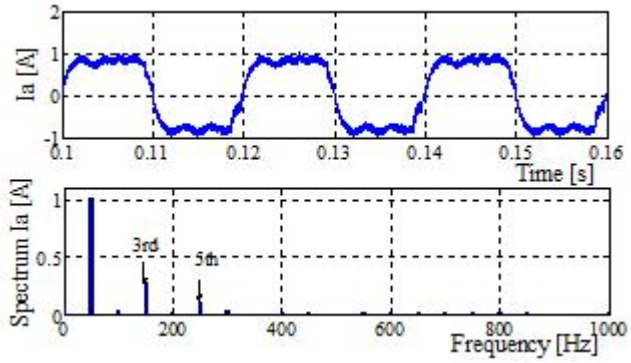



Fig. 8. Phase 'a' current time domain and frequency domain plots

### *B. Using $\gamma = 1, \delta = 1$ (current tracking in all three-planes) with 15 vectors*

Since the total harmonic distortion is high and is unacceptable, the tracking error is controlled in all the three planes by considering the tuning parameters equal to 1. In this case the number of vectors used remains the same and only tuning parameters is changed. The resulting waveforms are shown in Fig. 9-10. It is observed that the results improved significantly. The currents in x1-y1 and x2-y2 planes are reduced drastically when compared with Fig. 5b. The phase 'a' current is seen to be more sinusoidal. The THD has reduced to 5.03% considering upto 50th harmonics. This is acceptable limit.

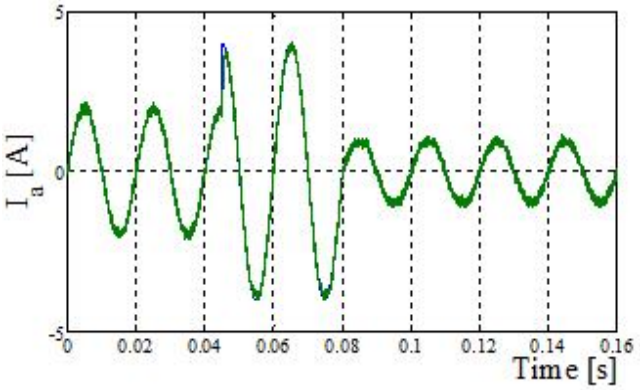



Fig. 9a. Actual and reference phase 'a' current for $\gamma = 1, \delta = 1$

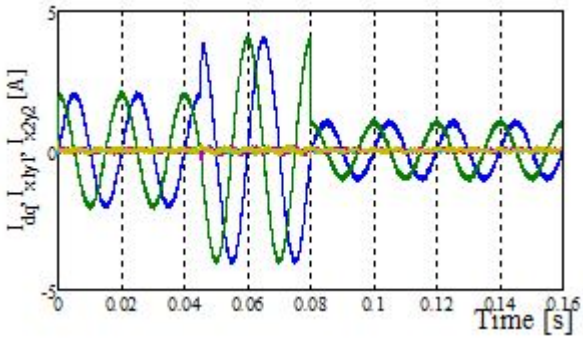



Fig. 9b. Transformed currents in d-q, x1-y1 and x2-y2 planes for $\gamma = 1, \delta = 1$

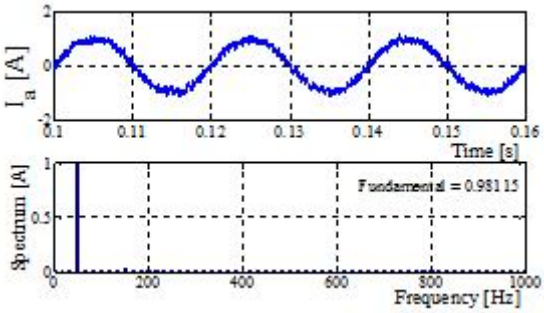



Fig. 10. Phase 'a' current time domain and frequency domain plots for $\gamma = 1, \delta = 1$ .

### *C. Using $\gamma = 1, \delta = 1$ (current tracking in all three-planes) with 29 vectors*

Further investigation is done by employing 14 more vectors from next large set. In this way total number of vectors used are 29 with 28 active and one zero as shown in Fig. 11.

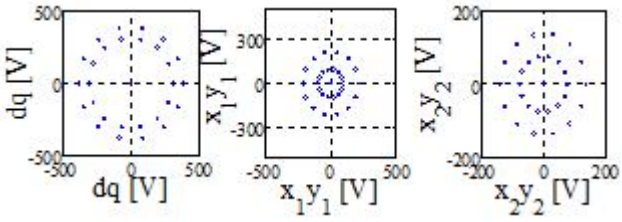



Fig. 11. Twenty eight vectors and their mapping.

Simulation parameters are kept the same and only change is in the number of space vectors. The resulting wavefors are shown in Fig. 12-13. It is observed that the reference current and actual current matches very well and the dynamics of control is fast. The x1-y1 and x2-y2 plane currents are reduced significantly. The THD is obtained for same upt 50th harmonic and is found to be 2.98%. This is an improvement over the 15 vectors case. When compared to the previous case of 15 vectors, it is a significantly improved performance in terms of much lower THD. Nevertheless, in the previous case of 15 vectors also the THD was within the specified limit of 5%. But the computational power required is more in the latter case.

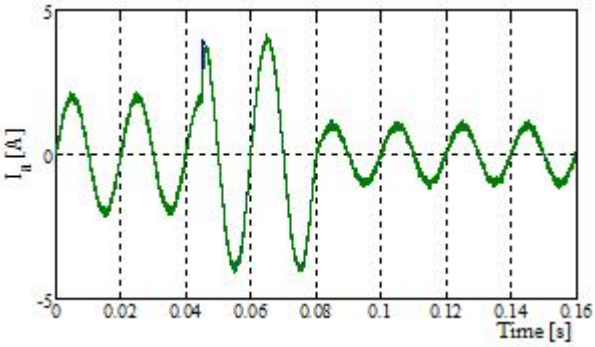



Fig. 12a. Actual and reference phase 'a' current for $\gamma = 1, \delta = 1$ and 29 vectors

© 2013 ACEEE
DOI: 03.LSCS.2013.4.9

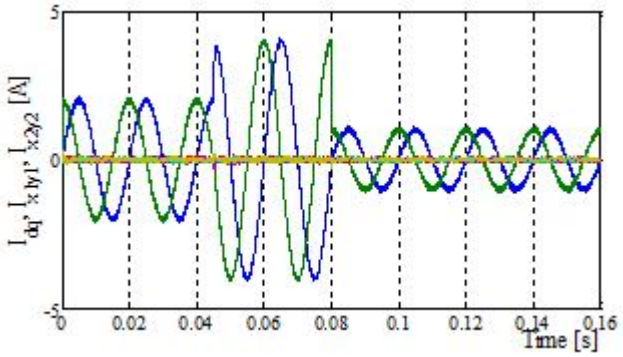



Fig. 12b. Transformed currents in d-q, x1-y1 and x2-y2 planes for $\gamma = 1, \delta = 1$ and 29 vectors

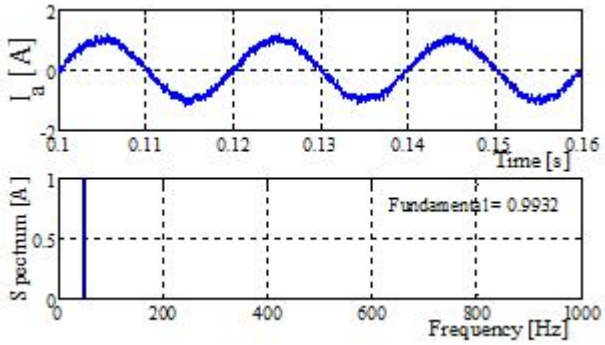



Fig. 13. Phase 'a' current time domain and frequency domain plots for $\gamma = 1, \delta = 1$ and 29 vectors

### *D. Using $\gamma = 1, \delta = 1$ (current tracking in all three-planes) with 43 vectors*

Fourteen additional vectors are added to the group for further investigation to look into the effect of more number of vectors on the total harmonic distortion. The 43 set of vectors with 42 active and one zero vector is shown in Fig. 14.

The spectrum of phase 'a' current for low frequency upto 1 kHz is depicted in Fig. 15. The current spectra shows a fundemental peak at 50 Hz as the fundamental component. The total harmonic distortion is now 2.65% which is well within the specified limit set by IEEE standard 519. It is important to note that the improvement in THD is too small and the computational power required in this case is comparitvely more.

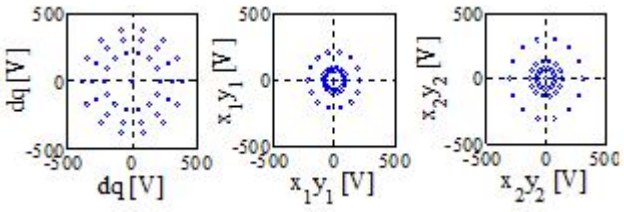



Fig. 14. 43 space vector and their mapping

## IV. Experimental Result

An experimental prototype seven-phase voltage source inverter is developed in the laboratory. The seven-phase inverter is controlled from dSpace 1006 in conjunction with

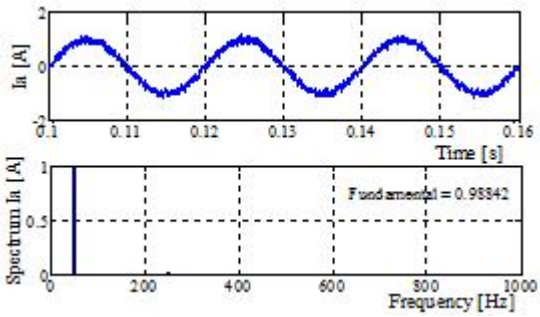
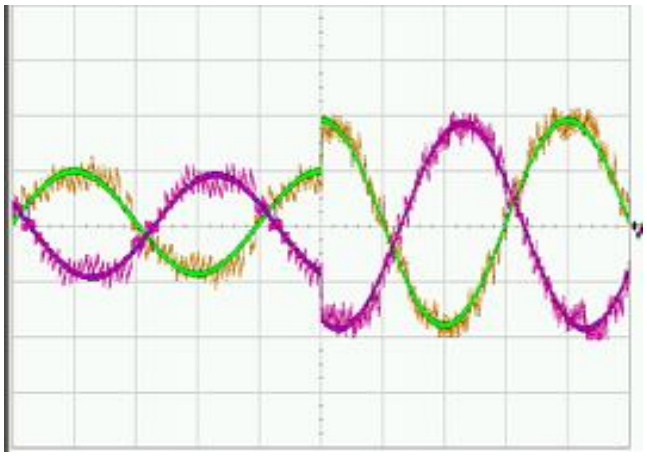
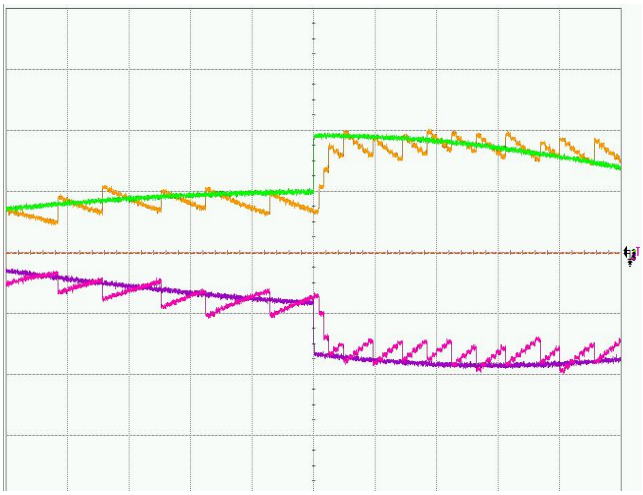



Fig. 15. Phase 'a' current spectrum for 43 space vectors

FPGA card DS 5203. The dSpace processor is connected with the FPGA card using PHS bus system. The control algorithm is written in the processor and the PWM signals are generated in the FPGA card. A dead band circuit is formulated outside the dSpace board based on FPGA and a dead band of 3 µs is created using VHDL. Sample time of 20 µs is used and a reference current of 1 A is chosen which is then stepped to 2 A with load impedance R = 75 &! and L = 33 mH. For experimental purpose, 29 space vectors are employed with control action on all three planes. The resulting waveform is shown in Fig. 16. The reference and actual currents are plotted in one waveform. A high dynamics of the control is evident and also a good tracking is obtained. This proves the viability of the proposed control.



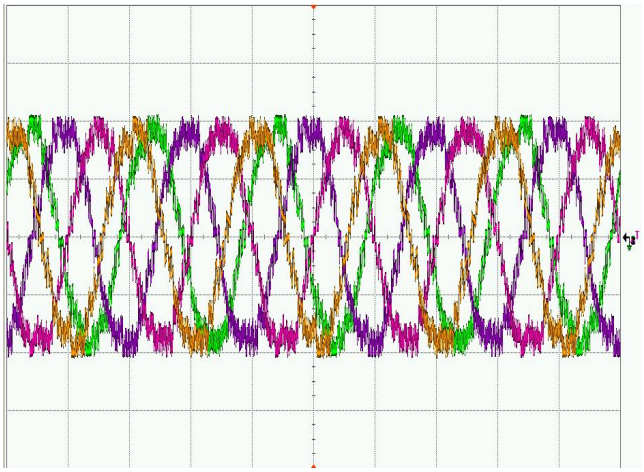
a.



b.

© 2013 ACEEE
DOI: 03.LSCS.2013.4.9

ACEEE



c.

Fig. 16. Experimental waveform for 7-phase MPC; a and b. dynamics, c. steady state condition

## V. Conclusion

The paper proposes current control technique based on finite set model predictive current control of a seven-phase voltage source inverter. The discrete time model of the load is used to predict the future behavior of the load current required in the next sampling interval. Space vector model of a seven-phase VSI is elaborated and out of 128 space vectors, three different scenario are investigated; a) 14 space vectors with control action on d-q plane only. This shows highly distorted current waveform with unacceptable limit of THD, b) 14 space vectors with control in three planes. The current shape become more sinusoidal and the THD reaches nearly 5%., c) 29 space vector are employed which yield improved results and the THD is close to 3%, d) finally 43 space vectors are used which give still better results but the improvement in terms of THD is not trivial. Hence it can be concluded that using 29 vectors is sufficient for getting better THD and good quality of waveforms and fast dynamics. In space vector PWM, 44 vectors (42 active and 2 zero) are needed to obtain sinusoidal waveform. While in proposed MPC only 29 vectors yield sufficiently good results.

## Acknowledgement

This publication was made possible by NPRP grant [4 - 077 - 2 – 028] from the Qatar National Research Fund (a member of Qatar Foundation). The statements made herein are solely the responsibility of the authors."

## References

[1] G.D. Holmes and T.A. Lipo, "Pulse Width Modulation for Power Converters - Principles and Practice," IEEE Press Series on Power Engineering, John Wiley and Sons, Piscataway, NJ, USA, 2003.

[2] M.P Kazmierkowski, R. Krishnan and F. Blaabjerg, "Control in Power Electronics Selected Problems", Academic Press, 2002.

[3] R. Ramchand, K. Gopakumar, C. Patel,K. Sivakumar, A. Das, and H. Abu-Rub "Online Computation of Hysteresis Boundary for Constant Switching Frequency Current-Error Space-Vector-Based Hysteresis Controller for VSI-Fed IM Drives", IEEE Trans. On Power Electronics vol. 27, no. 3, pp. 1521-1529, March 2012.

[4] A. Linder and R. Kennel, "Model Predictive control for electric Drives", Proc. 36th Annual IEEE PESC, Recife, Brazil, pp. 1793-1799, 2005.

[5] H. Abu-Rub, J. Guzinski, Z. Krzeminski and H. A. Toliyat, "Predictive current control of a voltage source inverters", IEEE Trans. On Ind. Elect., vol. 51, no. 3, pp. 585-593, June 2004

[6] H. Abu-Rub, A. Iqbal, J. Guzinski, "High performance control of AC Drives with Matlab/Simulink Models", Wiley, UK, 2012.

[7] J. Rodriguez and P. Cortes, "Predictive control of Power converters and electric drives", Wiley, UK., 2012.

[8] J.H. Lee, "Model predictive control: Review of three decades of development", Int. journal of Control Automation and System, vol. 9, no. 3, pp. 415-424, 2011.

[9] M. Jones and E. Levi; A literature survey of state-of-the-art in multiphase ac drives, Proc. 37th Int. Universities Power Eng. Conf. UPEC, Stafford, UK, 2002, pp. 505-510.

[10] A. Iqbal, H. Abu-Rub, SK. M. Ahmed, P. Cortes, and J. Rodriguez, "Finite state model predictive control of a five-phase VSI", Proc. IEEE ICIT, 2010.

[11] A. Iqbal, H. Abu-Rub, SK. M. Ahmed, P. Cortes, and J. Rodriguiz, "Model Predictive current control of a two-level five-phase voltage source inverter", Int. Journal of Applied Engineering Research, vol. 5, no. 21, pp. 3503-3514, 2010.

[12] F. Barrero, M.R. Arahal, R. Gregor, S. Toral and M.J. Duran, "A Proof of concept study of Predictive current control for VSI Driven Asymmetrical Dual three-phase AC machines", IEEE Tran. On Ind. Elect. Vol. 56, no. 6, pp. 1937-1954, June 2009.

[13] M.R. Arahal, F. Barrero, S. Toral, M. Duran and R. Gregor, "Multi-phase current control using finite state model predictive control", Control Engg. Practice, vol. 17, pp. 579-587, 2009.

[14] F. Barrero, M.R. Arahal, R. Gregor, S. Toral and M. Duran, "One Step Modulation Predictive current control method for asymmetrical dual three-phase induction machine", IEEE Trans. On Ind. Elect. Vol. 56, issue 6, 2009.

[15] J. Prieto, F. Barrero, M. Jones, and E. Levi, " A modified continuous PWM technique for asymmetrical six-phase induction machines", Proc. IEEE Int. Conf. on Ind. Tech. ICIT, pp. 1489-1494, 2010.

[16] A. Iqbal, H. Abu-Rub, SK. M. Ahmed, P. Cortes, and J. Rodriguez, "Finite state model predictive control of a three-level five-phase NPC inverter", Proc. IEEE 36th IECON, pp. 2953-2958, 2010.

[17] E. Levi, "Multi-phase Machines for variable speed applications", IEEE Trans. On Ind. Elect. vol. 55, no. 5, May 2008, pp. 1893-1909.

[18] A. Iqbal and E. Levi, "Space vector PWM techniques for sinusoidal output voltage generation with a five-phase voltage source inverter", Electric Power components and system, vol. 34, no. 2, pp. 119-140. 2006.

[19] S. Moinuddin and A. Iqbal, "Analysis of Space vector PWM techniques for a seven-phase VSI", I-Manger Journal of Engineering and Technology, vol. 1. No. 2., pp. 53-63, Oct-Dec. 2007

[20] S. Moinuddin, and A. Iqbal, "Modelling and Simulation of a seven-phase voltage source inverter", I-Manger Journal of Engineering and Technology, vol. 1, no. 1, July-Sept 2007, pp. 30-41.

© 2013 ACEEE

DOI: 03.LSCS.2013.4.9